



Evaluation of snow-surface energy balance models in alpine terrain

C. Fierz^{a,*}, P. Riber^{a,b}, E.E. Adams^c, A.R. Curran^d, P.M.B. Föhn^a,
M. Lehning^a, C. Plüss^a

^aWSL Swiss Federal Institute for Snow and Avalanche Research SLF, Fluelastrasse 11, Davos Dorf 7260, Switzerland

^bCentre National de Recherches Météorologiques Météo-France, F-31057 Toulouse Cedex, France

^cCivil Engineering Department, Montana State University-Bozeman, Bozeman, MT 59717, USA

^dThermoAnalytics, Inc., Calumet, MI 49913, USA

Abstract

The increasing complexity of snow-cover models demands high-quality forcing data. In complex alpine terrain, both short and long wave incoming radiation components are expected to be influenced by small-scale topographic effects, i.e. shading and multiple scattering as well as long-wave irradiance from the surroundings. Not only should the latter be included in distributed energy balance models, but, because of their increasing resolution, also in meteorological models of the next generation.

The energy balance at the snow-cover surface is calculated by means of different distributed energy balance models over a region of a few square kilometres, the spatial resolution being 25 m. The models include topographical effects on the radiation components of the energy balance. The region of interest is located in the Eastern Swiss Alps, around study sites of the Swiss Federal Institute for Snow and Avalanche Research SLF, Davos. The primary forcing data are taken from automatic weather stations located within the study area.

To assess performance and differences of the models, two approaches are taken. First, model outputs are compared to measurements of both incoming radiation and snow surface temperature measured at automatic weather stations located on either level or inclined terrain within the region. Second, the models are used to calculate snowmelt at the beginning of the ablation period. The results are compared with changes of the snow water equivalent as measured in various spots of the modelled region, including all aspects on one elevation range.

In view of the above comparison, the necessity to include small-scale topographic influences on the energy balance at the snow-cover surface as well as to consider snow surface properties and internal processes within the snow cover will be discussed. The possible implications for hydrological and meteorological models of the next generation will be addressed too.
© 2003 Elsevier B.V. All rights reserved.

Keywords: Snow; Alpine snow cover; Snow cover energy balance; Topographic effects; Snow melt; Snow cover simulation

1. Introduction

Mountainous topography is very complex even over small distances and thus the variability of the energy fluxes contributing to the energy balance of the snow cover is expected to be large. Because of

* Corresponding author. Tel.: +41-81-417-01-65; fax: +41-81-417-01-10.

E-mail address: fierz@slf.ch (C. Fierz).

logistical demand, it is difficult to perform a large number of measurements in complex terrain over either short or long time periods in order to measure the spatial variability of these fluxes. The most reasonable approach to obtain information about the energy fluxes in complex terrain is therefore a modelling approach that is verified by selected measurements at selected locations.

Motivated by the interest in snowmelt runoff at the scale of catchments, the main effort towards the modelling of the spatial distribution of the energy fluxes over snow covered surfaces was undertaken in snow hydrology (for a review, see Kirnbauer et al. (1994)). For instance, models taking account of shading or multiple scattering by surrounding terrain have long been proposed for both solar (e.g. Dozier, 1980) and long-wave radiation (e.g. Marks and Dozier, 1979). Due to even higher complexity, much less work has been done on the spatial distribution of turbulent fluxes, however. Though over longer periods of time their contributions to the energy balance may be minor, turbulent fluxes form an important part of the energy balance at daily and shorter time steps. Pre-requisite to a successful modelling of turbulent fluxes in steep alpine terrain are simulated wind fields with spatial resolutions corresponding to the digital elevation map used. This is a challenging task and puts a high demand on verification data to be collected in the field (Gauer, 2001; Doorschot et al., 2001).

Despite those modelling efforts, the WMO inter-comparison of models for snowmelt runoff (WMO, 1986) revealed that, with a typical time step of one day, the complexity level of snowmelt model structure could not be related to the quality of the simulation results.

Later on, investigating in detail the spatial distribution of the energy fluxes over snow covered mountainous surfaces, Plüss (1997) calculated as a case study the energy available for snowmelt over an alpine area of 16 km² during a one-month-period. He concluded that on shaded, inclined slopes, the energy available for melting is similar to the energy available on horizontal sites. This finding could only be explained by a major contribution of short and long-wave radiation from the surrounding terrain.

In addition, modelling glacier melt and discharge, Hock (1998) showed that, contrary to the WMO

study, in case of high resolution simulation with respect to space and time, model performance increased with higher model complexity. In particular, using hourly input data and considering the spatial distribution of radiation fluxes as well as long-wave terrain radiation, melt-induced daily discharge cycles could be well captured.

Unfortunately, snow-cover energy balance models are mostly restricted to applications to the main melt season, i.e. to so called ripe snow covers. Indeed, simulation of non-melt periods require considering internal processes within the snow cover. In order to simulate the evolution of initially subfreezing snow covers on adjacent north- and south-facing slopes, Fierz et al. (1997) used the output of Areal Energy Balance model (AEB; Plüss, 1997) to drive the detailed snow-cover model CROCUS (Brun et al., 1992). To do so, and despite most parameterisations used in the model were only verified for daily mean values, AEB was adapted to use and produce hourly input and output data. Although this procedure is not a proper full coupling of both energy balance and snow cover models, good qualitative agreement was found on both aspects between modelled and measured snow temperatures in subfreezing snow covers over a two-month period from 1 March to 2 May 1996.

Representing backgrounds as a collection of flat surfaces termed ‘facets’, Adams and McDowell (1991) provided a useful illustration of terrain effects in a topologically varied snow cover, showing strongly contrasting facets depending on size and orientation. Taking a further step along this line, the commercial product WinTherm/RT^{TM1} (Windows based Thermal model for Road Temperature) fully couples energy balance and snow cover simulation on each terrain facet of a given area. In addition, WinTherm/RT accounts for the effects of solar shadowing, reflections and long-wave irradiance by terrain features. A study aiming at the prediction of pavement temperature within complex topography showed this concept to be sound (Adams, 1999).

Very often high quality point measurements on level study sites are used to check model components separately. On larger scales, however, verification is mostly done by considering time and space

¹ Thermo Analytics, Inc., 94X Airport Road, Calumet, MI 49913, USA; <http://www.thermoanalytics.com>.

integrating measurements such as catchment discharge. This process of model verification involves that any inadequacies of the model will be lumped into tuned coefficients, leading eventually to a strong site dependency.

Recently, Gustafsson et al. (2001) conducted a model comparison over a flat arable field, showing the usefulness of such comparisons. Though their contribution to the energy balance cannot be neglected, turbulent fluxes will not be looked at in detail in this study due to a lack of reliable measurements. Therefore the present study aims at evaluating energy balance simulations over snow covered alpine terrain primarily with respect to their radiation components. Using ExtAEB, an extended version of AEB, emphasis is put on the relevance of an explicit coupling to the snow cover as well as on shading and scattering effects by the surroundings. Simulation results for both subfreezing and melting snow covers on either level or inclined terrain are compared to measurements performed in situ.

2. Description of models

2.1. The Areal Energy Balance model

The parameterisation of all components of the energy balance was combined by Plüss (1997) in a distributed energy balance model called AEB. AEB is primarily designed to deal with isothermal snow covers. A daily time resolution is considered accurate enough to investigate the variability of the energy fluxes due to different weather situations and for ablation modelling. The model calculates parameterised daily mean energy fluxes at the snow surface within a complex topography as given by a digital elevation map. The parameterisations are chosen in such a way that they are applicable with cloud cover observations and simple meteorological input data extrapolated from automatic weather station measurements, e.g. from either the newly implemented network of high Alpine automatic weather and snow stations IMIS² (Lehning et al., 1999) or the ANETZ³

network of MeteoSwiss, the Swiss Meteorological Institute.

Parameterisations of both the incoming short-wave and the incoming long-wave radiation fluxes from the sky are based on literature. Plüss (1997) showed them to be applicable to our study area. On the other hand, new parameterisations of albedo and surface temperature are derived from measurements performed on SLF's study site (cf. Fig. 1). Based on the concept of hemispheric fractions of both unobstructed and obstructed sky by terrain (Kondryatev, 1969), the modelling of the distributed radiation fluxes includes shading effects as well as reflection and emission by the surrounding topography. To parameterise the long-wave irradiance from the surroundings, an approach considering the influence of the air lying between emitting and receiving terrain surfaces is proposed (Plüss and Ohmura, 1996). Finally, parameterisation of the turbulent fluxes assumes for the drag coefficient calculated at the location of the automatic weather station to be constant over the study area and considers the bulk Richardson number as an indicator of stability. For the purpose of this study, a version predicting and driven by hourly data was used (Fierz et al., 1997).

2.2. ExtAEB

In order to be applicable to subfreezing snow covers, the energy balance needs to be solved explicitly and has to take into account internal processes within the snow cover. Consequently, Extended Areal Energy Balance model (ExtAEB) computes the energy balance iteratively on each grid point without using the surface temperature parameterisation introduced in AEB (Plüss, 1997). The energy balance includes effective heat conduction through a one-layer snow cover of given density and corresponding thermal conductivity, using the average temperature gradient taken over the full depth of the one-layer snow cover. Snow density ranges from 290 kg m^{-3} in winter to 420 kg m^{-3} in spring time, thermal conductivity from 0.24 to $0.41 \text{ W m}^{-1} \text{ K}^{-1}$, respectively. Under isothermal conditions, thermal conduction is limited to the top refreezing layer of the snow cover. Snow depth is varied according to precipitations and ablation only.

² German: Interkantonaless Mess- und Informations-System.

³ German: Automatisches Netz.

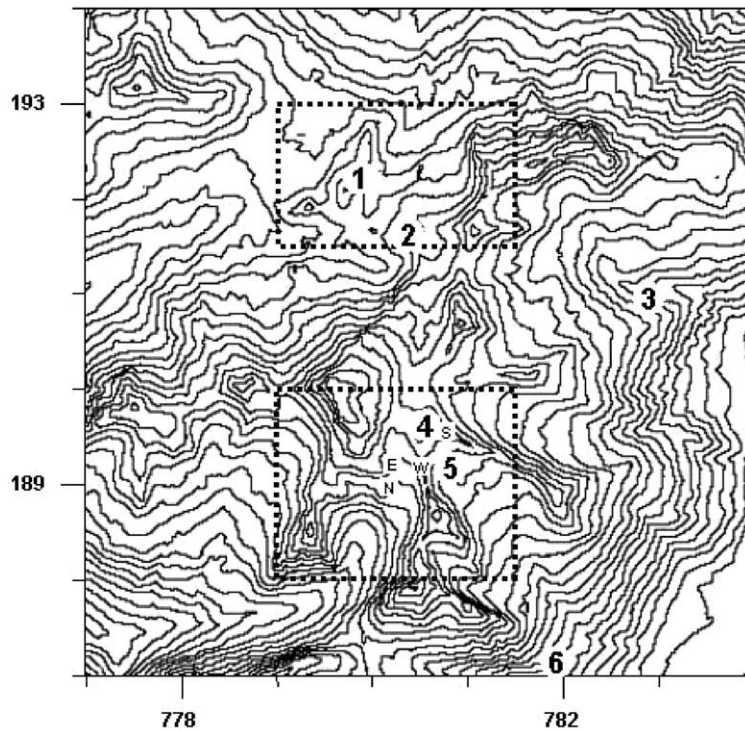


Fig. 1. Map of the studied area near Davos, in the eastern Swiss Alps. The number on the axes indicate the coordinate according to the Swiss kilometre grid. The contour interval is 50 m. The terrain data are based on a digital elevation map with a grid size of 25 m (DHM 25, © 2001 Bundesamt für Landestopographie, Swiss Federal Office of Topography). The figure covers the 7 km × 7 km area over which AEB and ExtAEB were run. The two boxes show the areas used with WinTherm/RT. (1) indicates the ridge of Gaudergrat, (4) the automatic weather station at Weissfluhjoch and (5) SLF's study site. Kreuzweg (2), Stützalp (3) and Büschalp (6) are additional level sites visited during the ablation period (May 99). The sites on slopes of varied aspects are marked by capital letters around (4) and (5).

Parameterisations of incoming radiation fluxes from both the sky and the surrounding terrain are implemented as in AEB, except for diffuse short-wave radiation from the sky, whose parameterisation is adapted to hourly input values (Erbs et al., 1982). Using the approach taken in AEB to parameterise turbulent fluxes, the iterative scheme does not converge under moderate wind conditions. Therefore, in ExtAEB, turbulent fluxes are computed assuming a neutral atmospheric surface layer and using Monin-Obukhov similarity theory (Lehning et al., 2002). Note that in our complex terrain setting, the assumption of a neutral atmospheric surface layer is justified over snow in the presence of moderate to high wind speeds. However, having no information about the snow-cover surface property, the iterative scheme described in Lehning et al. (2000) to solve for

the friction velocity and the roughness length cannot be used. Therefore, a fixed value of 10^{-3} m is used for the roughness length and the wind measurement height is set to 10 m above the snow cover.

3. Data

This study concentrates on three time periods of the winter 1998/1999. Data and periods will be described briefly below and Table 1 summarises where and how data were collected automatically during those periods.

3.1. Input data

The region studied is located in the Eastern Swiss Alps near the town of Davos, Switzerland.

Table 1

Summary of automatically measured input and verification data. Data from Gaudergrat not available during May 1999 (see text). AWS: automatic weather station belonging to MeteoSwiss; WRC: instruments belonging to the World Radiation Centre, Davos

	Weissfluhjoch (4 on Fig. 1)	SLF's study site (5 on Fig. 1)			Gaudergrat (1 on Fig. 1)	
	AWS	SLF	WRC	AWS	NW-slope	SE-slope
<i>Input</i>						
Air temperature	Ventilated					
Relative air humidity	Ventilated					
Wind	Pitot tube					
Global incoming solar radiation	Glass pyranometer Kipp and Zonen CM6					
Cloudiness (see text)	Observed					
Precipitation (see text)		New snow water equivalent		Rain gauge		
<i>Verification</i>						
Incoming solar radiation						
Direct			Pyrheliometer			
Diffuse			Shaded glass pyranometer			
Global			Glass pyranometer Kipp and Zonen CM21	Silicon pyranometer	Silicon pyranometer	
Reflected global solar radiation			Glass pyranometer Kipp and Zonen CM21			
Incoming long-wave radiation			Pyrgeometer Eppley PIR			
Snow surface temperature		Infrared thermometer		Infrared thermometer	Infrared thermometer	
Snow temperatures		20 cm-profile				

The Swiss Federal Office of Topography digital elevation map 'DHM25' with a grid size of 25 m is used to run both AEB and ExtAEB over the 7 km × 7 km region of interest. The same primary, hourly meteorological data feed into all models used. Air temperature, air humidity, wind, incoming global solar radiation are collected from the ANETZ⁴ automatic weather station located at Weissfluhjoch (4 on Fig. 1), 2693 m a.s.l. Precipitation is measured on SLF's study site (5 on Fig. 1), 2540 m a.s.l., i.e. daily recorded new snow water equivalent is distributed proportionally to

hourly readings of the automatic rain gauge located on the same site. Air temperature, air humidity and wind are height interpolated (Plüss, 1997). The phase of precipitation changes from solid to liquid at +1 °C and thus depends on altitude too. Other input data are taken as constant over the considered area. Incoming long-wave radiation from the sky is not routinely measured at either ANETZ or IMIS automatic weather stations. This flux is thus parameterised according to Plüss (1997), interpolating cloudiness at hourly steps from three cloud cover observations done daily at Weissfluhjoch. It is input to all models used and considered as constant over the calculation grid.

⁴ Automatic network of MeteoSwiss.

3.2. Verification data

The region of interest comprises two well equipped, high altitude study sites run by SLF: On the one hand SLF's level study site, on the other hand Gaudergrat (1 on Fig. 1), 2280 m a.s.l., a ridge with steep, adjacent north-westerly and south-easterly slopes.

3.2.1. Time periods

Two time periods extending over three days each were chosen to investigate the energy balance over subfreezing snow covers: First, from 19 to 21 January, 1999, second, from 10 to 12 February, 1999. Clear skies prevailed throughout the January period. The automatic weather station at Weissfluhjoch recorded air temperatures around -2°C , light winds ($1-6\text{ m s}^{-1}$) and a continuously diminishing relative air humidity. The February period was mostly overcast with no precipitations. Air temperatures around -20°C and moderate to strong winds (from 6 to 14 m s^{-1}) were recorded by the automatic weather station at Weissfluhjoch.

May 1999 was chosen to study energy balance over a melting snow cover. At the end of April 1999, snow temperatures were still slightly below freezing on SLF's study site while below 2100 m a.s.l., snow cover was ripe already. At Weissfluhjoch, May 1999 was characterised by light winds (rarely stronger than 4 m s^{-1}) and air temperatures mostly above freezing, except during a storm period from 20 to 23 May (moderate to strong winds up to 18 m s^{-1}). The latter brought about 144 mm of precipitation, which fell as snow down to 2200 m a.s.l. May 1999 was also a cloudy month: the sky was mostly overcast till the end of the storm period and still partially cloudy afterwards. It is assumed that all the terrain is snow-covered during all three-time periods. Except for a few, rather small rocky patches, this condition is fulfilled in January and February. However, this assumption may lead to errors during the melting period in May (cf. Section 4.3).

3.2.2. Radiation and snow-surface temperature measurements

On SLF's study site, high quality short and long-wave incoming radiation measurements are available from the World Radiation Centre/

Physical-Meteorological Observatory, Davos, WRC/PMOD (Marty, 2001). Despite its location on a rather broad valley bottom, measurable terrain effects on SLF's study site amount at most to 10 W m^{-2} for both short and long-wave irradiance (Marty, C., personal communication). Thus detailed verification of the incoming radiation fluxes from the sky may be performed at this site.

On the slopes of the remote Gaudergrat site, solely unventilated silicon type pyranometers are available to measure global solar radiation. Furthermore, on the north-westerly slope, the radiation sensor may be hit by direct solar radiation while snow surface is still fully shaded. Finally, on such steep slopes, it proved difficult to level the radiation sensors after initial installation. For all these reasons, only qualitative comparisons of simulated with measured short-wave radiation fluxes may be performed on Gaudergrat's slopes. Note also that in order to avoid damage by lightning, operation on Gaudergrat was discontinued by the end of April 1999. Extensive laboratory calibrations performed at SLF showed the infrared thermometers in use on our study sites to measure snow surface temperature within $\pm 1^{\circ}\text{C}$ (Weilenmann, 1998). Furthermore, comparison at SLF's study site over the three time periods of concern shows the measured snow surface temperature to be always lower, but at most 2°C , than the one inferred from measured outgoing long-wave radiation. Snow surface temperature measured on both level and inclined terrain will thus also be used for comparison purposes, though it represents the sum of all fluxes contributing to the energy balance over subfreezing snow-cover surfaces.

3.2.3. Snow water equivalent measurements

To assess the models overall performance on distributed snowmelt over the study area, snow water equivalent data were collected up to three times during May 1999: at the beginning and end of May on four slopes of varied aspects but similar altitude as SLF's study site (capital letters on Fig. 1); at the beginning, mid and end of May on SLF's study site, on a level site next to Gaudergrat (2 on Fig. 1), 2290 m a.s.l. and on two moderately inclined sites around 2000 m a.s.l., i.e. just above timber line (3 and 6 on Fig. 1).

4. Results and discussion

4.1. Incoming radiative fluxes

4.1.1. Detailed verification on SLF's study site

Ideally, one would like to check each flux of the radiation balance separately. This may be done on SLF's study site, where high quality radiation data are available. As stated above, terrain effects are usually

negligible on this site where horizon elevation is at most 19° towards NNW but less than 15° clockwise from NE to WNW. The hemispheric fraction of unobstructed sky calculated for SLF's study site being 1, no terrain effects are considered in ExtAEB either. Accordingly, parameterised incoming radiation fluxes from the sky are compared to measured direct and diffuse incoming short-wave solar radiation (Fig. 2) as well as incoming long-wave radiation (Fig. 3). On

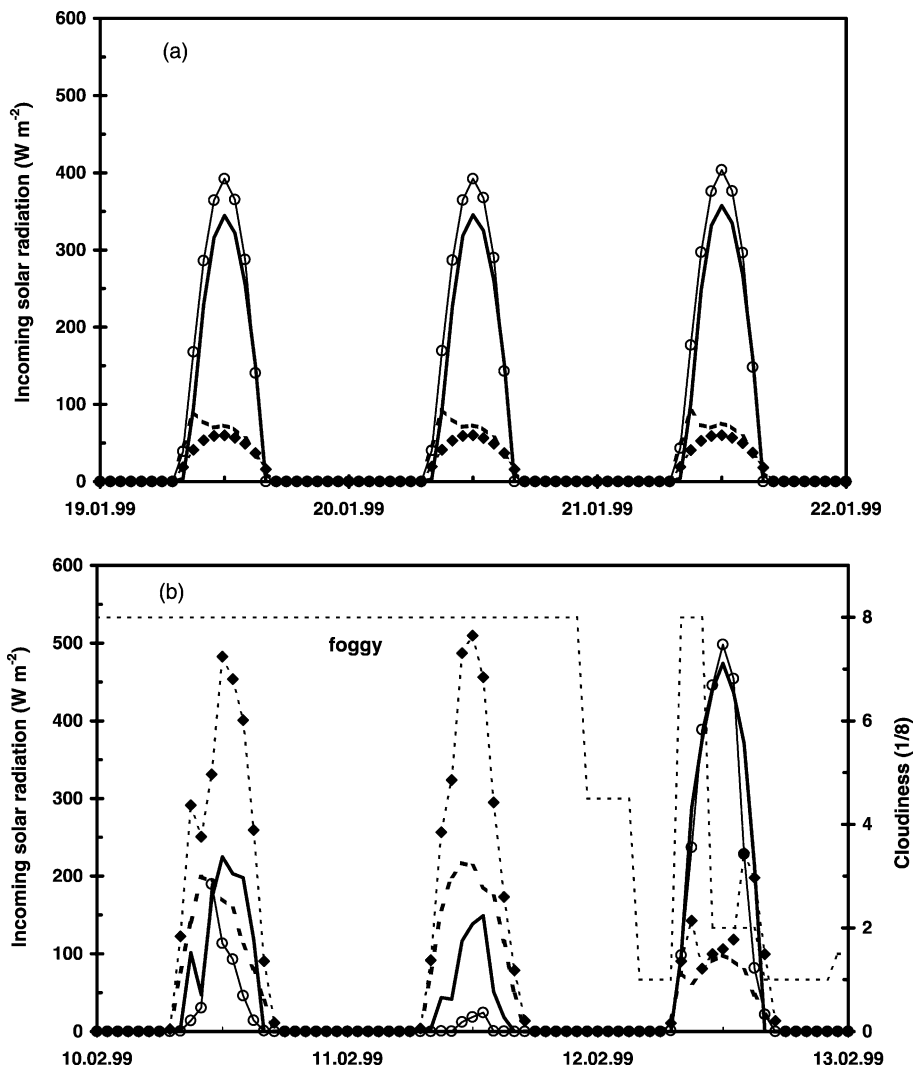


Fig. 2. Incoming solar radiation on SLF's study site for (a) the clear-sky period in January 1999; (b) the cloudy period in February 1999. Thick solid line and open circles are parameterised and measured direct solar radiation, respectively. Thick dashed line and closed diamonds are parameterised and measured diffuse radiation from the sky, respectively. Dashed line is interpolated cloudiness from three daily observations at Weissfluhjoch.

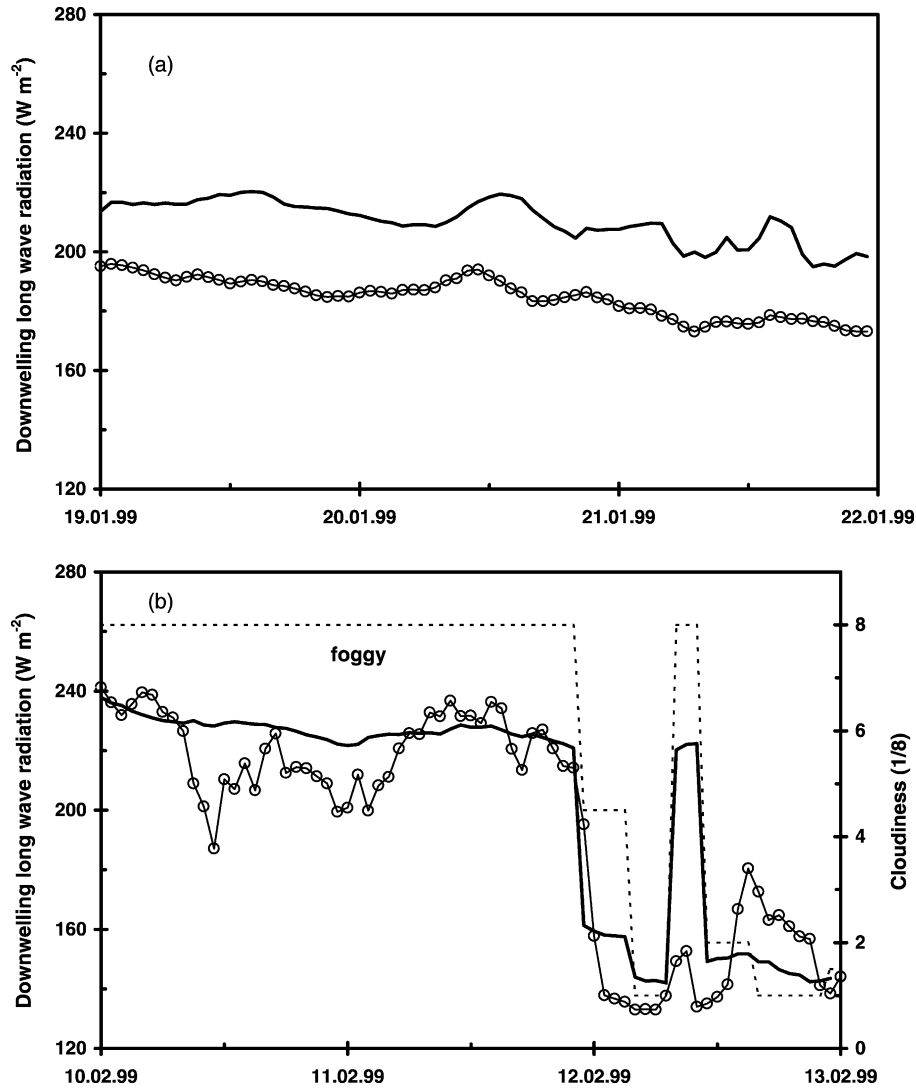


Fig. 3. Incoming long-wave radiation on SLF's study site for (a) the clear-sky period in January 1999; (b) the cloudy period in February 1999. Thick solid line and open circles are parameterised and measured incoming long-wave radiation, respectively. Dashed line is interpolated cloudiness from three daily observations at Weissfluhjoch.

clear sky days (19–21 January, 1999; Fig. 2a), both direct and diffuse solar radiation are well represented by ExtAEB. However, global radiation is constantly underestimated by about 30 W m^{-2} in January as well as in May. Part of this discrepancy may be attributed to model input and verification data being measured with different instruments (cf. Table 1), while the neglected terrain effects would account for the other part. Because of the high albedo of snow, the resulting

error on net radiation input to the snow cover is usually less than 7 W m^{-2} . While this error is negligible in May (cf. Section 4.3), it may not be the case during periods of low solar elevation such as January.

Whereas both direct and diffuse radiation are well represented on a partially cloudy day too (12 February, 1999; Fig. 2b), parameterised fluxes are far off on 10 and 11 February, 1999. Diffuse radiation,

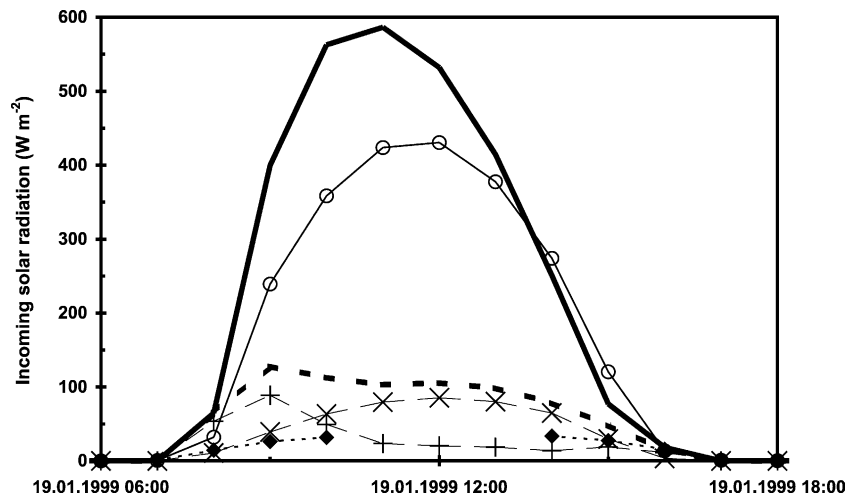


Fig. 4. Incoming solar radiation on the slopes of Gaudergrat. Thick solid line and open circles are parameterised and measured global radiation on the SE slope, respectively. Thick dashed line and closed diamonds are parameterised and measured global radiation on the NW slope, respectively. Straight crosses (+) and crosses (×) are parameterised diffuse radiation from the sky and from the surroundings on the NW slope, respectively.

for instance, is underestimated by a factor of up to 3. Both those days were characterised as foggy at the level of the automatic weather station, just above SLF's study site, while overcast conditions were reported at observation times (cloudiness of 8/8). Thus a thin, partly broken cloud cover is the most probable reason for this unexpected behaviour of diffuse radiation. Indeed, especially in mountainous terrain (multiple scattering), diffuse radiation will strongly depend on the homogeneity of the cloud cover (thickness, 'holes' etc) that is not considered in the parameterisations used.

Though the general trend of incoming long-wave radiation is quite well simulated, the observed and marked amplitude variations on 10 and 11 February confirm the above assumption of broken cloud cover too (Fig. 3b). As incoming long-wave radiation under clear sky and at constant air temperature depends primarily on water vapour pressure (Brutsaert, 1975), the decreasing amplitude of incoming long-wave radiation flux shown in Fig. 3a nicely reproduces the aforementioned drying up of the atmosphere. However, note that incoming long-wave radiation under clear sky is constantly overestimated by about 20 W m^{-2} .

4.1.2. Terrain effects on Gaudergrat

Irradiance by the surroundings is expected to play a role at Gaudergrat. Measured and simulated

global incoming short-wave radiation on both north-westerly and south-easterly slopes are shown on Fig. 4. As correctly predicted by ExtAEB, there is no incoming direct solar radiation on the shadowed north-westerly slope on 19 January 1999. Around midday, direct solar radiation hits the sensor sitting a few meters above ground, though. Accordingly, only measurements taken early morning and late afternoon represent the sum of diffuse radiation from both the sky and the surroundings. Obviously, in order to verify model results more accurately on slopes, more elaborate radiation measurements are needed, e.g. with attended sensors located near to the snow surface. Nevertheless, it appears clearly from Fig. 4 that diffuse radiation from the surroundings is strongly overestimated by ExtAEB. As the hemispheric fraction of obstructed sky by terrain is about 1.26 times larger on the south-easterly than on the north-westerly slope, overestimation of terrain effects explains to a large extent the marked mismatch of measured to simulated global radiation found on the south-easterly slope. Implementing the concept of view factors (Oke, 1987) is expected to improve modelling of solar shadowing, reflections and long-wave irradiance by surrounding terrain as compared with the obstructed and unobstructed fraction of hemisphere used in ExtAEB.

4.2. Snow surface temperature

Knowing from the above discussion how well some components of the radiation balance are predicted, it is interesting to look whether and how this reflects itself in the full energy balance. Over subfreezing snow covers, the latter is well represented by snow surface temperature, allowing to compare measured snow surface temperature with modelled energy balance expressed as surface

temperature. Furthermore, to show the importance of coupling to the snow cover, results from WinTherm/RT are included in this discussion. In the research version used for this study, energy balance and snow cover evolution simulated by the one-dimensional, finite element snow-cover model SNOWPACK (Lehning et al., 1999) are fully coupled on any user selected model facet. Due to higher computational demand, WinTherm/RT is run on two sub-grids (see Fig. 1).

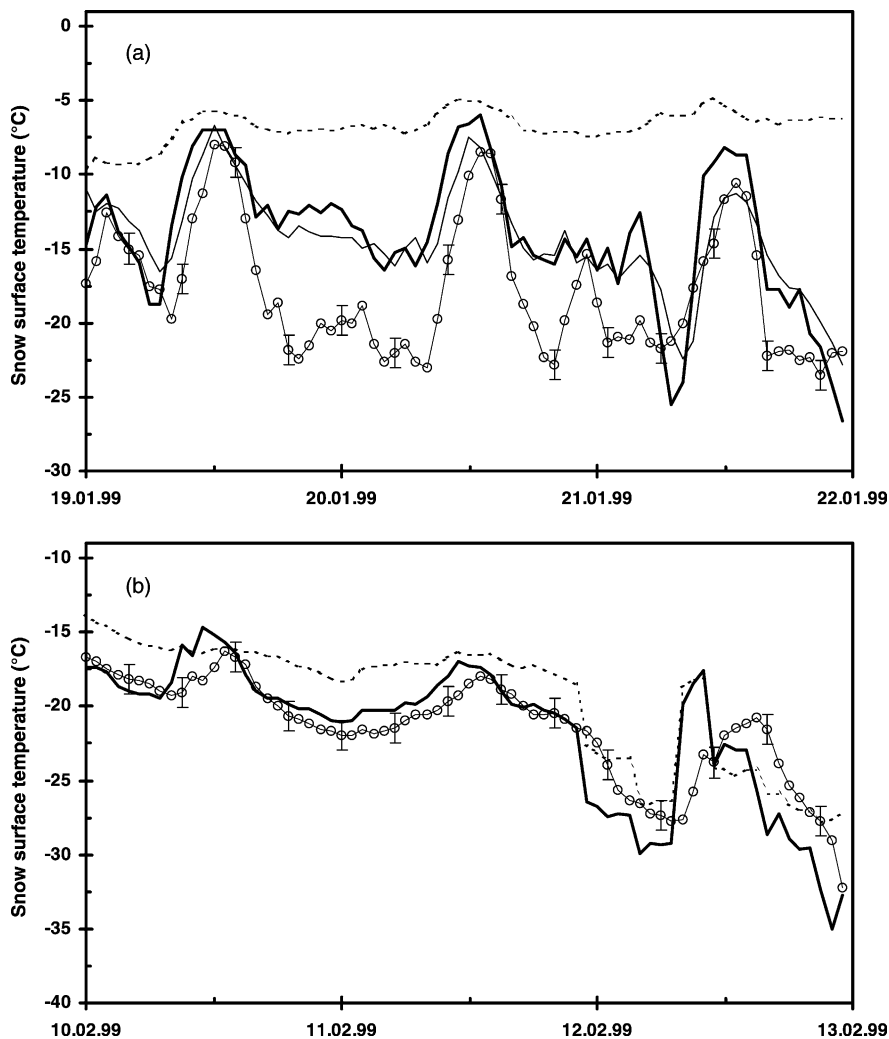


Fig. 5. Snow surface temperature on SLF's study site for (a) the clear-sky period in January 1999; (b) the cloudy period in February 1999. Open circles are measurements. Thick solid line and thin solid line are temperatures obtained from ExtAEB and WinTherm/RT (January only), respectively. Dashed line is the snow surface temperature as parameterised in AEB.

4.2.1. Dependency on slope and aspect

Fig. 5a and b show the comparison for SLF's study site during the January and February 1999 periods, respectively. First notice that the approach chosen in AEB strongly overestimates the snow surface temperature during the clear sky period in January while a good agreement is reached in February. As in AEB the parameterisation of snow surface temperature is based on air temperature and cloudiness only (Plüss, 1997), this underlines that a coupling to the subfreezing snow-cover is crucial during periods with partially cloudy skies. Indeed, the fully coupled model approach of

WinTherm/RT as well as the approach taken in ExtAEB both allow the marked diurnal cycle to be well captured in January. During this period, however, there is a marked discrepancy between measured and calculated surface temperature at night time. It may be attributed to the overestimation of the incoming long-wave flux shown in Fig. 3a. At daytime the overestimation of the long-wave flux is counterbalanced by the underestimation of incoming shortwave radiation (cf. Section 4.1), thus reducing the error's amplitude.

Fig. 6a and b show the comparisons for the January period on the north-westerly and south-easterly slopes

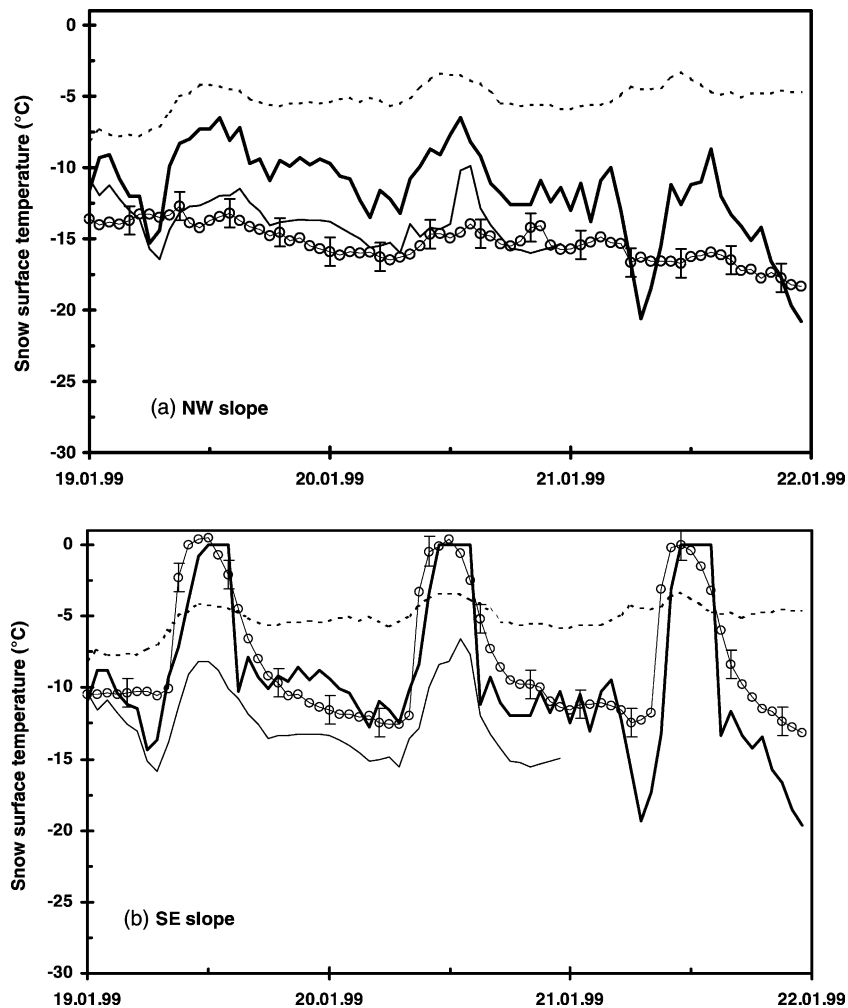


Fig. 6. Snow surface temperature on (a) the north-westerly and (b) the south-easterly slopes of Gaudergrat for the clear-sky period in January 1999. Open circles are measurements. Thick solid line and thin solid line are temperatures obtained from ExtAEB and WinTherm/RT, respectively. Dashed line is the snow surface temperature as parameterised in AEB.

of Gaudergrat, respectively. As expected from the chosen parameterisation of snow surface temperature, AEB shows no difference going from the north-westerly to the south-easterly slope. The difference in diurnal cycle and amplitude is well captured by both ExtAEB and WinTherm/RT, though. Because about 23 to 29% of the hemisphere is obstructed by terrain on Gaudergrat's slopes, overestimation due to incoming long-wave flux is obviously less pronounced here than on SLF's study site. On the other hand, note the exaggerated diurnal variation of snow surface temperature calculated by ExtAEB for Gaudergrat's north-westerly slope. Diffuse short-wave radiation by the surroundings being overestimated by ExtAEB (cf. Fig. 4), the latter energy flux may account for this discrepancy and possibly as well for the seemingly better agreement found for ExtAEB as compared to WinTherm/RT on the south-easterly slope (Fig. 6).

4.2.2. Effect of coupling on isothermal snow cover

Fig. 7 finally shows how surface temperature is represented over a mostly isothermal snow cover refreezing at night. While the AEB parameterisation does not follow many of the refreezing cycles, even not during the snow fall period from 20 to 23 May, 1999, a much better agreement is found for both ExtAEB and WinTherm/RT. However, although

ExtAEB includes a conduction flux within the uppermost 25 cm of the snow cover as the snow surface refreezes, it does not take into account phase changes near the surface and thus overestimates the amplitude of the nightly refreezing cycle at the surface. In this respect, the fully coupled approach of WinTherm/RT performs slightly better, showing once again that processes internal within the snow cover must be explicitly included to obtain best results. Indeed, simple rules of the thumb do not work properly in such cases, as shown by Hock (1998). Neglecting such processes may be of less importance to long term hydrological studies, however, as shall be seen below, they may account for some quantifiable errors.

4.3. Detailed evaluation of possible errors on snowmelt at SLF's study site

Next the snowmelt period in May 1999 is considered. While above 2400 m a.s.l. the assumption of all terrain being covered by snow does hold throughout May, between 2000 and 2400 m a.s.l. only 50–60% of the terrain may have been snow covered towards the period's end and even less below 2200 m a.s.l. However, because air efficiently screens off the effect of surface temperature on the long-wave radiation emitted by terrain (Plüss and Ohmura,

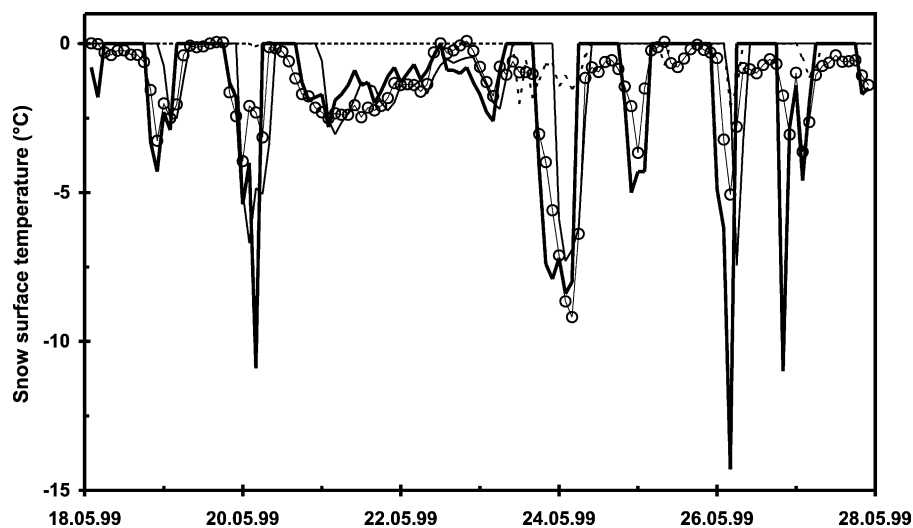


Fig. 7. Snow surface temperature on SLF's study site during a period in May 1999. Open circles are measurements. Thick solid line and thin solid line are temperatures obtained from ExtAEB and WinTherm/RT, respectively. Dashed line is the snow surface temperature as parameterised in AEB.

1996), the additional energy input will be negligible (Plüss, 1997). Moreover, as less short-wave radiation will be reflected by the same terrain patches, the additional incoming radiation flux from surrounding terrain will be further reduced. In summary, this additional radiation flux as well as advective energy fluxes from nearby bare patches are neglected, though they could certainly affect results for sites below 2400 m a.s.l.

An usual approach to compute snowmelt implies that, as snow surface temperature reaches 0 °C, any surplus of energy at the surface-air interface will be immediately used for melting. Fig. 8 shows the cumulative snowmelt energy Q_m as computed by ExtAEB for SLF's study site, converted to snow water equivalent SWE (units: mm) according to:

$$\text{SWE} = Q_m / L_f \quad (1)$$

where L_f is latent heat of fusion. Measured changes ΔHW in snow water equivalent from 4 to 17 May and 4 May to 1 June, 1999, respectively are represented by filled squares. Note that ΔHW is corrected for solid precipitation, i.e. the sum of new snow water equivalents is added to the actually measured change in total snow water equivalent for the corresponding period. Also shown are cumulative rain and new snow

water equivalents. Obviously, measurements and simulation do not quite match.

4.3.1. Sources of errors

Whenever simulation predicts available melt energy on SLF's study site, possible erroneous contributions δswe to snowmelt for each component of the energy balance may be analysed separately. In Table 2, these errors are summed up over a period of interest, subtracted from the predicted cumulative snowmelt amount ΔSWE for the same period and the result compared to the measured changes ΔHW . For radiation fluxes, δswe is the difference of simulated to measured flux converted to snow water equivalent. For global incoming solar radiation, errors due to differences between parameterised and measured albedo are also considered. In addition, internal processes within the snow cover have to be considered: on the one hand cold content, that is the energy required to warm up a subfreezing snow cover to 0 °C (e.g. at the beginning of May and after the snowfall), on the other hand phase changes, that is melt-freeze processes within the uppermost layers of the snow cover. While the former is considered by using automatically measured snow cover temperatures with a vertical resolution of 20 cm, the latter may only be approximated qualitatively. It is assumed

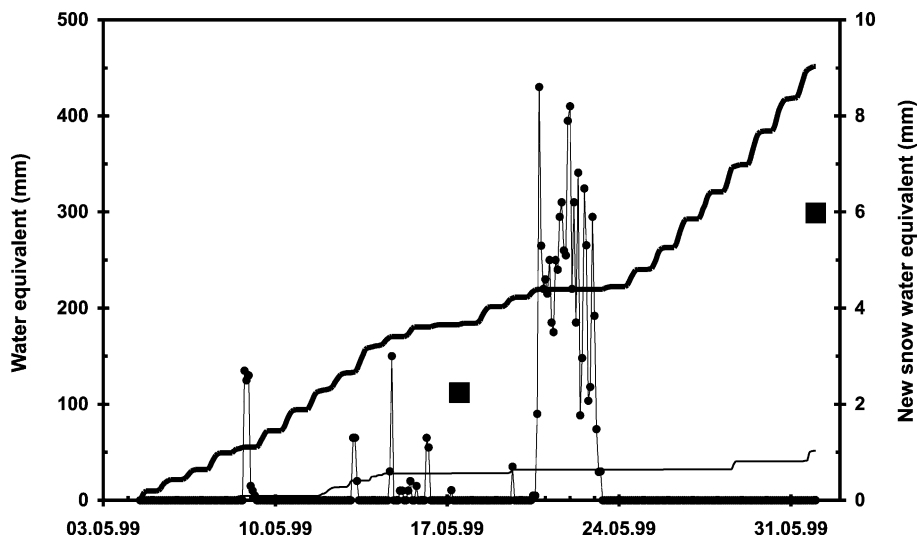


Fig. 8. Snowmelt on SLF's study site during May 1999. Thick solid line is cumulative snowmelt calculated by ExtAEB. Closed squares are measured changes in snow water equivalent. Dots are measured new snow amounts and thin solid line is cumulative rain.

Table 2

SLF's study site, May 1999: measured changes in snow water equivalent (ΔHW), computed cumulative snowmelt amount (ΔSWE) and errors due to various components of the energy balance (δs_{we}), all in mm water equivalent

From To	Time period					
	04.05.99 12:00 17.05.99 12:00	17.05.99 12:00 01.06.99 00:00	04.05.99 12:00 12.05.99 00:00	12.05.99 00:00 17.05.99 12:00	17.05.99 12:00 23.05.99 00:00	23.05.99 00:00 01.06.99 00:00
Mean cloudiness (1/8)	6.6	5.4	6.2	7.2	7.3	4.2
New snow water equivalent (mm)	19	145	8.4	10.5	142.2	2.7
ΔHW measured (corrected for precipitations)	112	187				
ΔSWE ExtAEB	183	269	114.7	68.1	36.5	232.0
δs_{we} due to long-wave irradiance	5	36	5.8	-0.4	0.5	35.2
δs_{we} due to global radiation	-1	-8	-1.4	0.4	-2.0	-6.2
δs_{we} due to albedo	14	23	10.9	3.0	-0.5	23.7
ΔSWE ExtAEB (corrected for radiation fluxes)	165	218	99.4	65.1	38.5	179.3
δs_{we} due to cold content	3	2	3.0			2.0
δs_{we} due to phase changes (8 h)	25	20	12.5	12.5	7.5	12.5
ΔSWE ExtAEB (corrected additionally for phase changes)	137	196	83.9	52.6	31.0	164.8
δs_{we} due to sensible heat flux	9	11	3.8	4.9	3.6	6.9
δs_{we} due to latent heat flux	3	2	0.0	2.7	-0.4	2.6
ΔSWE ExtAEB (corrected additionally for turbulent fluxes)	125	183	80.1	45.0	27.8	155.3

that, on the average, surface temperature must be below freezing for eight hours in order to refreeze a 10 cm thick layer of wet snow at the surface. Then, the so-called irreducible water content (about 2.5 vol%) must be reached in that layer before melt starts again. The required snowmelt energy per melt-freeze cycle thus corresponds to 2.5 mm snow water equivalent, a relative small amount. For turbulent fluxes, no measurements are available to compare with. Thus the difference of the fluxes as calculated by ExtAEB to those predicted by AEB is computed. Because the corrections implied by this analysis would affect in turn the calculation of the energy balance, the results summarized in Table 2 are a first approximation only.

4.3.2. Considering sub-periods in may 1999

Let's consider first the two periods from 4 to 17 May and 17 May to 1 June, 1999. From Table 2, it is obvious that errors due to radiation fluxes contribute substantially to the mismatch. Note, however, that global incoming radiation, as mentioned previously

(see Section 4.1 and Fig. 2), is slightly underestimated, resulting in a negative error to the energy balance. Nevertheless, without taking into account internal processes such as phase changes, no reasonable agreement is reached with the measured snow water equivalent changes.

Even better results are obtained by considering possible errors due to turbulent fluxes. Indeed, because predicted surface temperature is better captured in ExtAEB (see Fig. 7), sensible heat flux is expected to be larger than its counterpart in AEB and leads therefore to additional positive errors on the energy balance. This last statement must be kept in perspective as the lack of corresponding measurements does not allow to assess the computation of either the flux itself or parameters such as roughness length. A better knowledge of the latter would require a full coupling to the snow cover, though.

Let's get one step further. In Table 2, 4 sub-periods are considered, showing under which conditions what error may arise. As shown in Fig. 9, daily mean

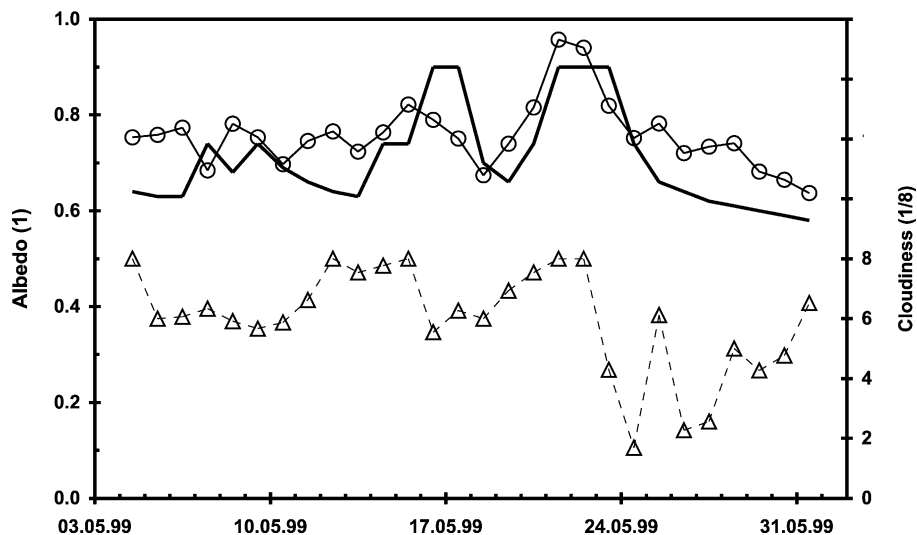


Fig. 9. Daily mean values for albedo and cloudiness on SLF's study site during May 1999. Thick solid line and open circles are parameterised (ExtAEB) and measured albedo, respectively. Open triangles are cloudiness.

cloudiness was mostly less than 6/8 from 23 to 31 May, 1999. Incoming long-wave radiation being overestimated under clear sky (see Fig. 3), this incoming flux contributes heavily to the mismatch during this last period with fair weather: the lower the mean cloudiness, the larger the error.

Albedo underestimation also contributes to the mismatch, particularly after the storm period from 24 May to 1 June 1999. During this period, measured albedo was constantly higher than its parameterised counterpart (cf. Fig. 9). Indeed, albedo parameterisation in ExtAEB does not include explicitly grain size and grain shape. Snow albedo, however, shows a strong dependence on the latter parameters (see e.g. Warren, 1981; Brun et al., 1992; Lehning et al., 2002).

Contrary to this, errors due to the parameterisation of incoming global solar radiation fluxes are slightly negative, irrespective of the time period and in agreement with our previous findings.

Finally, contributions from neglected phase changes must be considered during all four periods.

In summary, one important source for errors is linked to the parameterisation of incoming long-wave irradiance from the sky while two other important sources for errors are related to components of the energy balance intimately linked to the snow cover, i.e. albedo and phase changes.

4.4. Inter-site comparison of snowmelt

4.4.1. Level sites at various altitudes

For the period from 4 May to 1 June 1999, Fig. 10 shows a comparison of measured and simulated water equivalent changes on four different level sites at various elevation. At about 2000 m a.s.l., on Büschalp and Stützalp, the match between simulation and measurements is somewhat better than at higher elevations. Indeed, at this elevation, errors due to neglecting phase changes account for only about 50% of those found at the level of SLF's study site and shown in Table 2. Moreover, albedo parameterisation may better fit snow surface conditions found at 2000 m a.s.l. as little new snow fell during the storm period and snow cover was ripe beginning of May already. This further demonstrates that processes intimately linked to the properties of the snow cover must be accounted for in order to study snowmelt events under any prevailing conditions.

4.4.2. Various aspects at similar altitude

Fig. 11 shows the results of both ExtAEB and AEB for the four aspects at the elevation of the study site (see Fig. 1) over the period from 4 May to 1 June 1999. First note that no measurements were performed mid-May on those sites. Second, the north slope where

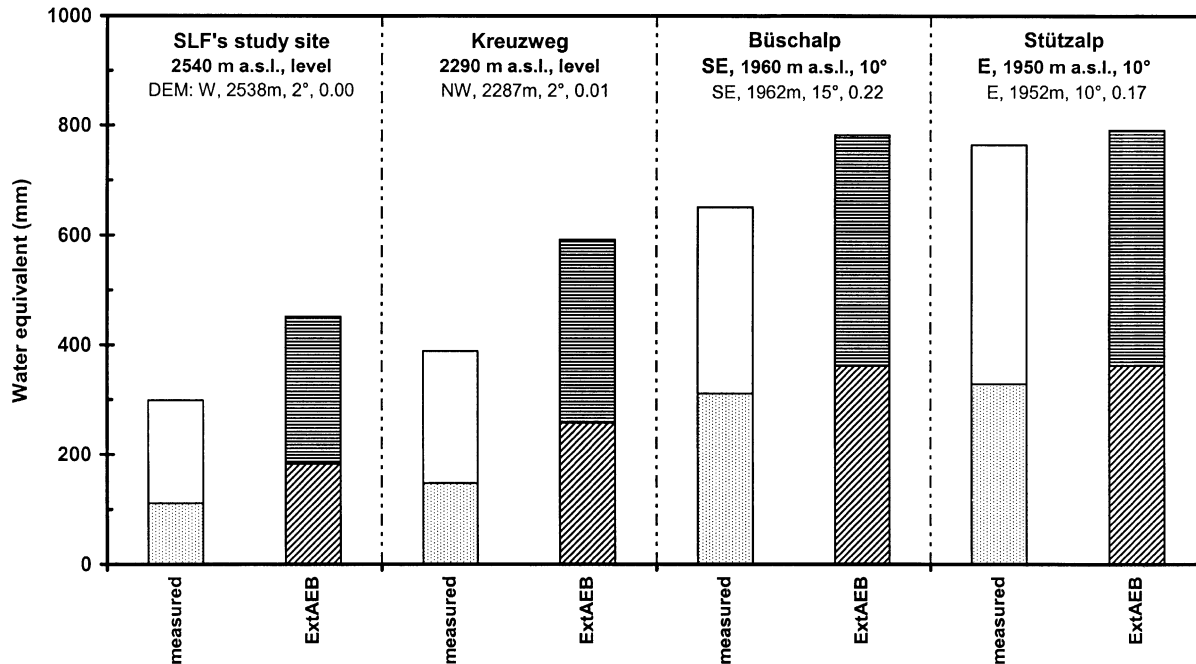


Fig. 10. Measured changes in snow water equivalent (ΔHW) and computed cumulative snowmelt (ΔSWE) for May 1999 on level sites at varied elevations. The lower part of the columns represent the period from May 4 to May 17, the upper part from May 17 to June 1. Measured aspect, elevation and exposition are given in bold for each site; corresponding values from the digital elevation map (DEM) as well as the fraction of sky obstructed by terrain used by ExtAEB are noted underneath.

measurements were taken is too small to be accounted for by the digital elevation map and the comparison is made with the best fitting model slope nearby. However, the north-easterly exposition of the latter leads to non negligible direct solar radiation flux which reflects itself in a large mismatch between measurement and simulation. Thus, particularly along ridges and for small terrain features, inaccuracies of the digital elevation map can lead to serious problems and one has to take this into account too. Third, AEB and ExtAEB yield comparable results, ExtAEB predicting slightly more snowmelt. In Section 4.3, many possible sources of errors, which may account for the discrepancy between measured and modelled changes in total snow water equivalent at the elevation of SLF's study site were discussed in detail. Nevertheless, note that observed trends are qualitatively reproduced by the model. For instance, both measured and simulated changes in snow water equivalent are significantly lower on an easterly slope than on a westerly slope across the valley (see Fig. 1).

Given the aspect and inclination of these two slopes, one would not expect such a difference. The latter, however, may be due to the fraction of obstructed sky by terrain, which is twice larger on the westerly than on the easterly slope. On the other hand, redistribution of new snow by wind is not accounted for by any of the models used and this may be another explanation for the discrepancy found on slopes.

5. Conclusions

The type of model one selects to study energy balance over snow covers depends on the intended purpose and, in particular, on the amount of input data available. As high resolution meteorological models start to emerge, data availability will no longer restrict the use of sophisticated snow cover energy balance models to well equipped study areas. Moreover, full coupling to snow cover

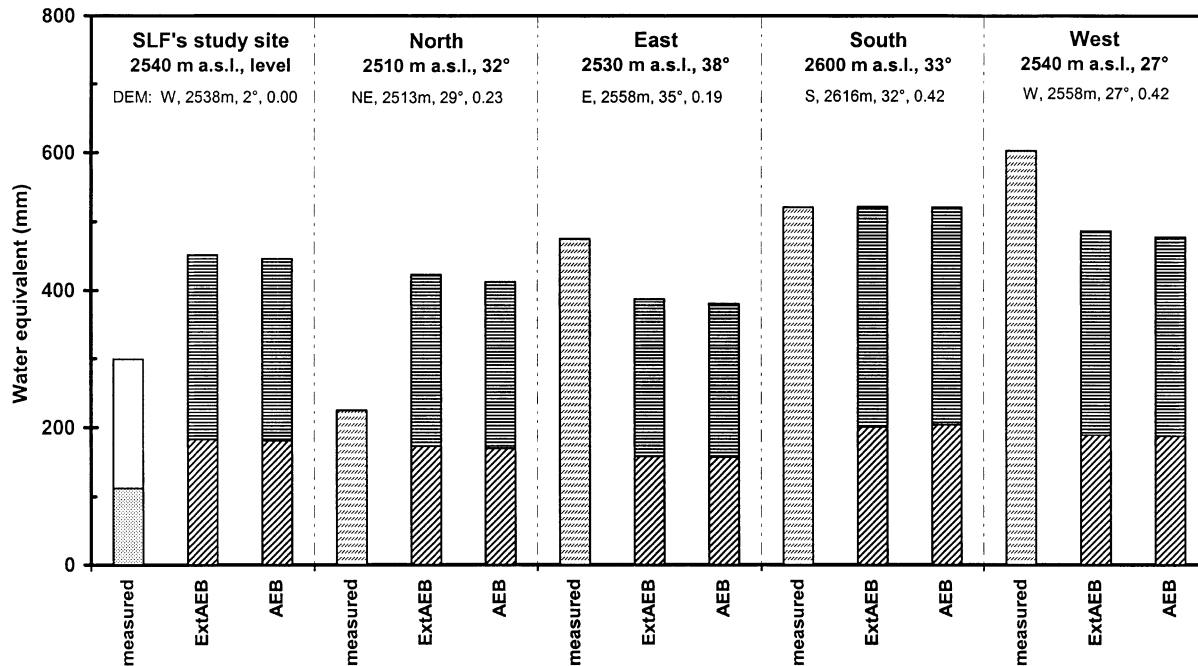


Fig. 11. Measured changes in snow water equivalent (ΔHW) and computed cumulative snowmelt (ΔSWE) for May 1999 on slopes with varied aspects at the elevation of SLF's study site. The lower part of the columns represent the period from May 4 to May 17, the upper part from May 17 to June 1. Note that on slopes measurements were only taken on May 4 and on June 1. Measured aspect, elevation and exposition are given in bold for each site; corresponding values from the digital elevation map (DEM) as well as the fraction of sky obstructed by terrain used by both ExtAEB and AEB are noted underneath.

models does not increase data requirements and has to be considered in order to obtain good model performance under any nivo-meteorological conditions. Not only do we need to account for surface properties to model properly albedo (radiation) or roughness length (turbulent fluxes), but internal processes such as heat conduction through the snow cover and phase changes within the snow cover have to be included. The good agreement between results obtained either from ExtAEB, which includes some coupling to the snow cover, or from WinTherm/RT, a fully coupled model, confirms this to be especially true for subfreezing snow covers indeed, but also at the beginning of an ablation period, as the above analysis of snow water equivalent changes during May 1999 shows.

In ExtAEB, incoming solar radiation from an unobstructed sky is reasonably well parameterised, except for particular cloud cover situations. Generally

speaking, independently of cloudiness, direct solar radiation is slightly underestimated whereas diffuse solar radiation from the sky is overestimated and shows much more scatter. Usually, however, direct solar radiation is much larger than diffuse radiation from the sky and thus incoming global solar radiation is quite well captured. Parameterising albedo independently from snow cover properties leads to large errors in particular after substantial snow falls on an otherwise ripe snow cover. Finally, a qualitative comparison with measurements from a shadowed slope shows that diffuse short-wave radiation from the surroundings is markedly overestimated. Clearly, terrain effects need to be included but must be investigated further in order to get more realistic parameterisations.

Incoming long-wave radiation is consistently overestimated by a factor of about 20 W m^{-2} for cloudiness lower than $4/8$. Accordingly, whenever this energy flux dominates the energy balance, e.g. at

night, the computed outgoing long-wave radiation flux is too large. This leads, e.g. to overestimated temperatures at the surface of subfreezing snow covers. A better parameterisation must thus be sought.

The goal of our future efforts is first to improve ExtAEB regarding small-scale topographic influences on the energy balance at the snow-cover surface by introducing view factors and taking account of properties that vary from one aspect to another. Second, the detailed snow cover model SNOWPACK will be coupled to the energy balance calculation in order to take properly account of processes within the snow cover. Furthermore, surface properties predicted by SNOWPACK will affect both radiation and turbulent fluxes. Though this coupling will increase model complexity, no additional input data will be needed, a crucial point for many applications, e.g. hydrological ones. In addition, more work will have to be put towards a better verification of both predicted radiation and turbulent fluxes in steep alpine terrain.

Finally, advances in energy balance modelling over snow covered surfaces will also benefit meteorological models of the next generation which will have to include effects as multiple scattering of solar radiation and long-wave irradiance from terrain.

Acknowledgements

The authors would like to thank W. Ammann for his interest in this work and his continuing support. This work would not have been possible without the help and assistance of O. Bauer, T. Baunach and S. Harvey during the May 1999 measurement campaign. We also thank WRC/PMOD Davos for providing the high quality data from their radiation instruments located on SLF's study site. One of us (P. Riber) would like to thank MétéoFrance for giving her the opportunity to do her 'stage d'approfondissement' at SLF. We are indebted to our colleagues J. Rhyner, M. Stähli and J. Schweizer for their comments on the manuscript. Finally we thank two anonymous reviewers whose insightful work helped to greatly improve the manuscript's readability.

References

- Adams, E.E., 1999. Proof of concept for prediction of pavement temperature: a tactical decision aid for highway safety. Final report FHWA/MT-99-003/8117-6 to the state of Montana Department of Transportation and the US Department of Transportation Federal Highway Administration.
- Adams, E.E., McDowell, S.A., 1991. Thermal model for snow on three dimensional terrain. Proceedings of Japan–US Symposium on Snow Avalanche, Landslides, Debris Flow Prediction and Control, Tsukuba, Tsukuba-shi, Ibaraki-ken, September, 1991, Japan.
- Brun, E., David, P., Sudul, M., Brugnot, G., 1992. A numerical model to simulate snow-cover stratigraphy for operational avalanche forecasting. *J. Glaciol.* 38, 13–22.
- Brutsaert, W., 1975. On a derivable formula for long wave radiation from clear skies. *Water Resour. Res.* 11, 742–744.
- Doorschot, J., Raderschall, N., Lehning, M., 2001. Measurements and one-dimensional model calculations of snow transport over a mountain ridge. *J. Glaciol.* 32, 153–158.
- Dozier, J., 1980. A clear sky spectral solar radiation model for snow-covered mountaineous terrain. *Water Resour. Res.* 16, 709–718.
- Erbs, D.G., Klein, S.A., Duffie, J.A., 1982. Estimation of the diffuse radiation fraction for hourly, daily and monthly-average global radiation. *Sol. Energy* 28 (4), 293–304.
- Fierz, C., Plüss, C., Martin, E., 1997. Modelling the snow cover in a complex alpine topography. *Ann. Glaciol.* 25, 312–316.
- Gauer, P., 2001. Numerical modelling of blowing and drifting snow in Alpine terrain. *J. Glaciol.* 47 (156), 97–110.
- Gustafsson, D., Stähli, M., Jansson, P.-E., 2001. The surface energy balance of a snow cover: comparing measurements to two different simulation models. *Theor. Appl. Climatol.* 70, 81–96.
- Hock, R., 1998. Modelling of Glacier Melt and Discharge, *Zürcher Geographische Schriften*, Heft 70, Zürich, 126 pp.
- Kirnbauer, R., Blöschl, G., Gutknecht, D., 1994. Entering the era of distributed snow models. *Nord. Hydrol.* 25 (1/2), 1–24.
- Kondryatev, K.Y., 1969. Radiation in the atmosphere, Academic Press, New York, San Francisco, London, p. 912.
- Lehning, M., Bartelt, P., Brown, R.L., 1999. Snowpack model calculations for avalanche warning based upon a new network of weather and snow stations. *Cold Reg. Sci. Tech.* 30, 145–157.
- Lehning, M., Doorschot, J., Bartelt, P., 2000. A snow drift index based on SNOWPACK model calculations. *Ann. Glaciol.* 31, 382–386.
- Lehning, M., Bartelt, P., Brown, R.L., Fierz, C., Satyawali, P.K., 2002. A physical SNOWPACK model for avalanche warning services. Part III: meteorological boundary conditions and applications. *Cold Reg. Sci. Tech.* 35 (3), 169–184.
- Marks, D., Dozier, J., 1979. A clear-sky long wave radiation model for remote alpine areas. *Arch. Met. Geophys. Biokl.* 27, 159–178.
- Marty, C., 2001. Surface radiation, cloud forcing and greenhouse effect in the Alps, *Zürcher Klima-Schriften*, 79, Verlag Institut für Klimaforschung ETH, Zürich, 122 pp.

- Oke, T.R., 1987. Boundary layer climates. Routedledge, 2nd ed., p. 435.
- Plüss, C., 1997. The energy balance over an alpine snowcover: point measurements and areal distribution, Zürcher Geographische Schriften, 65, Verlag Geographisches Institut ETH, Zürich, 115 pp.
- Plüss, C., Ohmura, A., 1996. Longwave radiation on snow-covered mountainous surfaces. *J. Appl. Meteor.* 36, 818–824.
- Warren, S.G., 1981. Optical properties of snow. *Rev. Geophys. Space Phys.* 20 (1), 67–89.
- Weilenmann, P., 1998. Messungen mit der IR-Thermometer Eichenanlage [Calibrating Infra Red Thermometer], Interner Bericht, 702. Swiss Federal Institute for Snow and Avalanche Research, 132 pp.
- WMO, 1986. Intercomparison of models for snowmelt runoff. Operational Hydrology Report 23 (WMO No. 646).